

Numerical Investigation of Nonlinear Interactions between Multimodal Guided Waves and Delamination in Composite Structures

Yanfeng Shen*

University of Michigan-Shanghai Jiao Tong University Joint Institute, Shanghai Jiao Tong University, Shanghai, 200240, China

ABSTRACT

This paper presents a numerical investigation of the nonlinear interactions between multimodal guided waves and delamination in composite structures. The elastodynamic wave equations for anisotropic composite laminate were formulated using an explicit Local Interaction Simulation Approach (LISA). The contact dynamics was modeled using the penalty method. In order to capture the stick-slip contact motion, a Coulomb friction law was integrated into the computation procedure. A random gap function was defined for the contact pairs to model distributed initial closures or openings to approximate the nature of rough delamination interfaces. The LISA procedure was coded using the Compute Unified Device Architecture (CUDA), which enables the highly parallelized computation on powerful graphic cards. Several guided wave modes centered at various frequencies were investigated as the incident wave. Numerical case studies of different delamination locations across the thickness were carried out. The capability of different wave modes at various frequencies to trigger the Contact Acoustic Nonlinearity (CAN) was studied. The correlation between the delamination size and the signal nonlinearity was also investigated. Furthermore, the influence from the roughness of the delamination interfaces was discussed as well. The numerical investigation shows that the nonlinear features of wave delamination interactions can enhance the evaluation capability of guided wave Structural Health Monitoring (SHM) system. This paper finishes with discussion, concluding remarks, and suggestions for future work.

Keywords: structural health monitoring, guided waves, nonlinear ultrasonics, composite structures, LISA, delamination, higher harmonics

1. INTRODUCTION

The prompt detection and quantification of delamination in composite structures is critical for the prevention of catastrophic failures. Ultrasonic guided waves have been investigated as a promising interrogation tool to achieve real-time passive and active structural sensing. When guided waves interact with the delamination, Contact Acoustic Nonlinearity (CAN) may arise due to the clapping of the delamination interfaces, which may introduce distinctive signal features such as higher harmonics and side-band frequency components. Thus, the nonlinear ultrasonic phenomena possess great potential to improve the delamination evaluation capability of current Structural Health Monitoring (SHM) systems.

The evolution of damage in composite structures undergoes several stages, such as matrix cracking, matrix-fiber debonding, delamination, and fiber breakage. During such a procedure, the damage are mostly hidden underneath the laminate surface and are hard to notice. Conventional linear ultrasonic inspection techniques are only sensitive to relatively large size damage. On the other hand, nonlinear ultrasonic techniques have shown much higher sensitivity to incipient structural changes with distinctive nonlinear features, such as sub/higher harmonic generation, DC response, mixed frequency modulation response (sideband effects), and various frequency/amplitude dependent threshold behaviors [1]. The integration of nonlinear ultrasonic techniques into guided wave based inspection procedures is drawing increasing attention from the SHM and Nondestructive Evaluation (NDE) communities, because such a practice inherits both the sensitivity from nonlinear techniques and the large-area inspection capability from guided waves [2]. Many researchers have explored using guided waves for delamination detection. Utilizing the linear information of guided waves and scanning laser vibrometry, delamination was detected with advanced signal processing techniques [3, 4]. Research efforts aiming at taking advantage of the nonlinear information during wave delamination interaction have been reported as well. Soleimanpour et al. investigated the higher harmonic generation at the delamination and utilized nonlinear guided waves to locate the delamination zones in laminated composites [5, 6]. Yelve et al. also conducted finite element modeling and experiments to apply nonlinear ultrasonic methods to detect delamination [7, 8].

*yanfeng.shen@sjtu.edu.cn, Phone: +86-21-34206524, Fax: +86-21-34206525

To investigate the CAN, various modeling approaches have been developed. Analytical models are computationally efficient and allow fast parametric studies, but are confined by the complexity of structures and damage types [9]. To fully capture the 3-D nonlinear dynamics, finite element method (FEM) for contact-impact problems has been widely investigated, maturing over the years [10]. But the handling of massively large matrices inevitably result in heavy cost of computer resource and computational time even for explicit solving schemes. Moreover, the proper choice of contact parameters to achieve solution convergence and accuracy is always found to be challenging and tedious, which requires extensive modeling experience. Time domain Boundary Element Method (BEM) has been explored as an efficient approach to solving CAN by considering a boundary-type nonlinear problem, in which the nonlinear effect is contained in the boundary conditions only [11]. Finite Difference (FD) method was also investigated for contact-impact analysis of crack surfaces with much less computational burden compared to conventional FEM [12]. To solve wave propagation in heterogeneous materials, the Local Interaction Simulation Approach (LISA), based on FD formulation and Sharp Interface Model (SIM), has been developed. 1-D, 2-D, and 3-D LISA formulations were first developed for isotropic heterogeneous materials executed on Connection Machines [13, 14, 15]. LISA underwent considerable progress during the past decade, with its extension to general anisotropic materials [16], coupled field capabilities [17], hybridization with other numerical methods [18, 19], and execution on powerful Graphics Processing Units (GPU) with Compute Unified Device Architecture (CUDA) technology [20]. Pioneer research on including nonlinear effects into LISA formulation has been conducted using a spring model in 1-D, 2-D, and 3-D cases [21, 22, 23]. This spring model LISA formulation altered the material at the crack location between continuous and discontinuous status to simulate the crack close and open phenomena during wave crack interaction. Recently, Shen and Cesnik put forward a new LISA formulation with contact dynamics and investigated the nonlinear interactions and mode conversions of guided waves at fatigue cracks [24].

In this study, the 3D LISA formulation with contact dynamics is applied to simulate the nonlinear interactions between guided waves and delamination. Several guided wave modes at various frequencies were investigated as the incident wave. Numerical case studies of different delamination locations across the thickness were carried out. The capability of different wave modes to trigger the CAN was studied. The correlation between the delamination size and the signal nonlinearity was investigated. A nonlinear resonance phenomenon associated with delamination size was presented. Furthermore, the influence from the roughness of the delamination interfaces and nonlinear wave amplitude effect were also discussed.

2. LOCAL INTERACTION SIMULATION APPROACH WITH CONTACT DYNAMICS

This section outlines the theoretical fundamentals of LISA and the methodology of introducing CAN into the LISA formulation. The parallel implementation using CUDA technology accelerated on GPU device is also presented.

2.1 Local Interaction Simulation Approach (LISA)

LISA is a finite-difference based numerical simulation method. It approximates the partial differential elastodynamic equations with finite difference quotients in the discretized temporal and spatial domains. The coefficients in LISA iterative equations (IEs) depend only on the local physical material properties. The SIM enforces the stress and displacement continuity between the neighboring computational cells and nodes. Therefore, changes of material properties in the cells surrounding a computational node can be captured through these coefficients. The final IEs determine the displacements of a certain node at current time step based on the displacements of its eighteen neighboring nodes at previous two/three time steps, depending on whether material damping is considered. For details of the derivation for the LISA IEs, the readers are referred to Ref. [16].

2.2 Adding contact dynamics into LISA

A penalty method was deployed to introduce contact dynamics into LISA. Penalty method was initially investigated to solve a class of constrained optimization problems and have been adopted as one of the primary approaches to simulate contact problems in FEM. It approximates a constrained problem by an unconstrained one whose solution ideally converges to the solution of the original constrained problem. Its convergence is achieved by punishing the violation of these constrains.

In the context of contact analysis, the impenetrability condition in contact continuum mechanics is weakened, which means a small amount of penetration is allowed to enable the mathematical formulation. This penetration can be easily identified as the measurement of violation against the impenetrability condition and is penalized by introducing a contact stiffness that tends to minimize this violation. When an appropriate contact stiffness is reached, the amount of penetration approaches zero, which makes the numerical solution converges towards the physical contact phenomena. A typical

contact procedure during wave delamination interaction can be categorized into four consecutive stages: (1) pre-contact state, where the contact surfaces are separate from each other and are subjected to free boundary conditions; (2) contact initiation, where contact counterparts meet, which triggers the exertion of contact forces; (3) in-contact motion, where the delamination surface moves together in a stick-slip pattern, with interactive contact forces; (4) contact pair separation, where the contact counterparts leave each other, releasing the contact interactions and regaining the free boundary conditions. It can be noticed that the boundary condition of the contact surfaces alters between free and constrained situations.

To satisfy the alternating boundary conditions at the contact surfaces, special design and treatment of the computational grid are needed. In this study, a discontinuous mesh is used to model the delamination interfaces. The structural discretization was carried out using the commercial FEM software ANSYS 14 preprocessor. Then, a model converter was programmed using CUDA C to convert the nodal connectivity and material allocation from the FEM format to that of LISA. During such a conversion procedure, three additional steps were taken to prepare the LISA computational grid for the contact analysis, including contact pair recognition, normal direction detection, and auxiliary air cell addition. It should be noted that the air cells on the contact surfaces are not implemented during structural discretization in ANSYS but are generated during the model conversion procedure. When the delamination surfaces come into contact, penalty contact forces are acted on the contact nodes to constrain the in-contact motion. Thus, the modeling of the alternating boundary condition can be achieved. A Coulomb friction model is integrated to simulate stick-slip contact motion. The details of the nonlinear contact LISA formulation and the guidelines for the proper choice of computational parameters for an accurate and converged solution are given in Ref [24].

2.3 CUDA implementation for parallel computing on graphic cards

In this study, the contact LISA algorithm was implemented using CUDA technology and executed in parallel on GPUs (NVIDIA GeForce Titan with 2688 CUDA cores and 28672 concurrent threads). There are two major characteristics of the current contact LISA formulation that enables the computation to be expedited. First, LISA is massively parallel: the computation of a general node or a contact node only depends on the solutions of its eighteen neighboring nodes at the previous two time steps. The behavior of each node is independent from the others at the target time step, facilitating LISA's readiness for parallel computing. Second, the wave simulation tasks usually require dense discretization of the structure, resulting in a computationally intensive problem. GPUs, with their massive concurrent threading feature, are suitable to handle such large size problems by distributing the workloads among a large number of functional units and carry out highly efficient parallel computing. During the computation, the parameters are first established in the host memory (RAM). Then a copy of these parameters is sent to the device memory (GPU global memory) for it to be processed. The computation of each node is assigned to a functional thread, i.e., each thread gathers the displacements of its eighteen neighboring nodes and one contact pair node (if identified as a contact node) at previous two time steps, process the material properties in the eight surrounding cells, and execute the kernel to compute the displacements of this node at the target time step. Since one of the bottlenecks of a CUDA program is the data transfer between the device memory and host memory, results are transferred from the GPU to the CPU only sporadically (every 10-30 steps depending on the frequency upper bound of the interested propagating waves) to minimize such data transfer cost.

3. THE LISA MODEL FOR STUDYING WAVE DELAMINATION INTERACTIONS

This section will first present the guided wave characteristics in the unidirectional CFRP laminate used for study. Then, the detailed description of the LISA model is given.

3.1 Guided waves in the unidirectional carbon fiber composite plate

The composite laminates used in this study were manufactured from pre-impregnated composite tape made from IM7 fibers and Cy-com 977-3 resin. The total thickness of the plate is 4 mm. The mechanical properties of the lamina were given in Table 1.

Table 1: Mechanical properties of the IM7/977-3 ply.

E_{11} (GPa)	E_{22} (GPa)	E_{33} (GPa)	ν_{12}	ν_{13}
147	9.8	9.8	0.41	0.41
ν_{23}	G_{12} (GPa)	G_{13} (GPa)	G_{23} (GPa)	ρ (kg/m ³)
0.48	3.7	3.7	3.31	1558

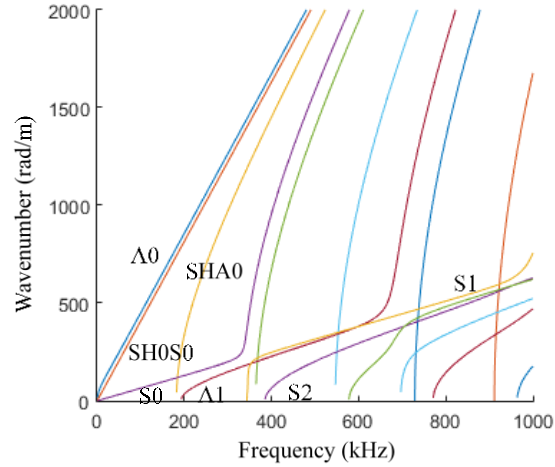


Figure 1: Dispersion curves of guided waves in the 4-mm thick unidirectional laminate composite plate.

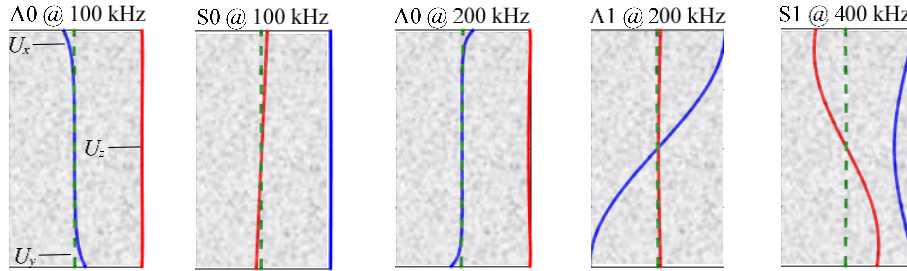


Figure 2: Mode shapes of guided waves at various frequencies in the laminate composite plate.

A Semi-Analytical Finite Element (SAFE) method was used to compute the dispersion curves and the modes shapes associated with the guided waves in the unidirectional CFRP laminate composite plate. Figure 1 shows the frequency-wavenumber dispersion curves along the fiber direction. The multimodal and dispersive characteristics of plate guided waves are quite obvious. It should be noted that S0 wave possesses a much longer wavelength and a much higher propagation speed than A0 wave mode. During a linear interaction between guided waves and the structural damage, the sensing signals will only contain the frequency components of the excitation, i.e., if an excitation centered at f_c is used, then the response will only show the same frequency components centered at f_c in the sensing signals. However, for a nonlinear system, distinctive higher harmonics may appear at $2f_c$, $3f_c$, $4f_c$, etc. Thus, beyond the cut-off frequencies, complex mode conversion may happen between the fundamental modes at the excitation frequency and the high order wave modes at the higher harmonics.

Figure 2 presents the mode shapes of various wave modes at several frequencies of interest. It can be noticed that A0 mode undergoes large out-of-plane motion, while the in-plane deformation is very small. On the other hand, S0 mode possesses dominant in-plane motion, while the out-of-plane deformation is quite small. Unlike A0 showing dominant out-of-plane motion, A1 mode at 200 kHz, however, has dominant in-plane deformation and minor out-of-plane motion. The mode shape of S1 at 400 kHz shows obvious motion in both in-plane and out-of-plane direction. The mode shape information is especially important for choosing appropriate excitation profiles to generate corresponding wave modes. In-phase or anti-phase surface traction forces can be applied to couple with certain mode shapes and achieve the effective generation of selective wave modes.

3.2 LISA model layout

The LISA model tailored to study the nonlinear interactions between guided waves and delamination is presented in Figure 3. A 500-mm long, 40-mm wide, and 4-mm thick unidirectional composite strip was modeled. The fiber orients along x direction. Two lines of forces at top and bottom of the composite strip, parallel to the in-plane direction, were used to selectively generate certain guided wave mode into the structure, i.e., in-phase excitation will induce symmetric wave

modes and anti-phase excitation will induce anti-symmetric wave modes. The delamination locates 100 mm away from the wave source. The guided waves generated by the line traction forces will propagate along the composite strip, interact with the delamination, and are finally picked up at the sensing locations. Two kinds of representative delamination scenarios are studied, namely middle delamination (at half the plate thickness) and edge delamination (at a quarter of the plate thickness). Its size a was assigned with different values to investigate the influence of damage size on the signal nonlinearity. A line of sensing points were used to record the wave signals and perform frequency wavenumber analysis, so that the wave modes in the response can be revealed. Absorbing Layers with Increasing Damping (ALID) was implemented at both ends of the composite strip to eliminate the influence from boundary reflections [25]. The LISA models used in this study adopts the in-plane cell size of 0.5 mm in x direction, 1 mm in y direction, and a through-thickness cell size of 0.5 mm. The time step according to the Courant-Friedrichs-Lewy (CFL) condition is 33.35 ns, which corresponds to a CFL number of 0.99.

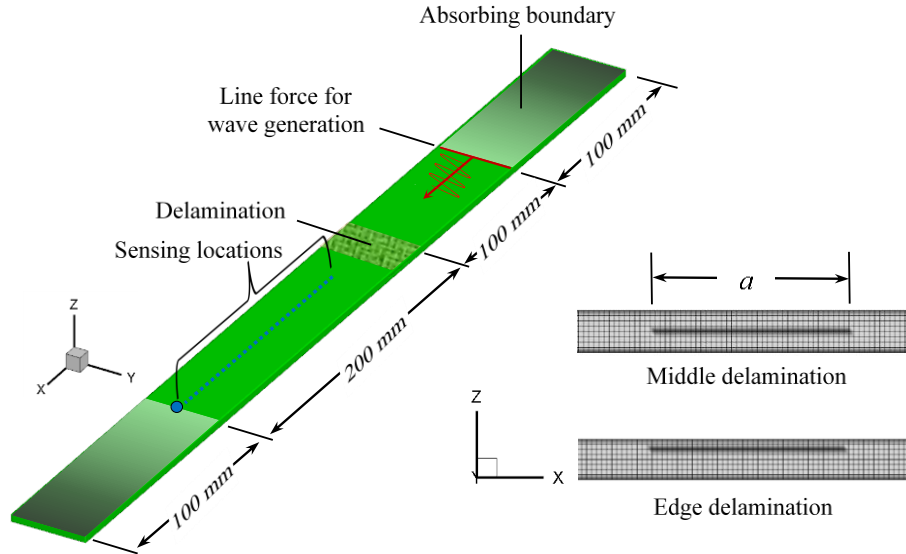


Figure 3: LISA model and grid for studying nonlinear interactions between guided waves and delamination.

4. NUMERICAL RESULTS

After laying out the fundamentals of the LISA model, numerical case studies will be presented on the nonlinear phenomena introduced by the interaction between guided waves and delamination. Various guided wave modes at different frequencies were studied. The effect of the delamination location and size on the nonlinearity of the sensing signals was investigated. A random distribution of initial openings and closures at the delamination interface was considered and the effect of excitation amplitude on the wave nonlinearity was discussed.

4.1 Selective wave mode interaction with middle delamination

Figure 4 presents the simulation results of the two fundamental modes, S_0 and A_0 , being generated, propagating along the laminate strip, and interacting with the delamination. A 100 kHz 10-count tone burst excitation was used to generate the guided waves. From the dispersion curves shown in Figure 1, only fundamental wave modes may exist as incident waves. It can be noticed that S_0 waves propagate with a long wavelength. After it interact with the delamination, trapped mode can be noticed within the delamination region. The effective absorption of wave energy at the ALID boundary can be observed. On the other hand, A_0 waves propagate in the laminate strip with a much smaller wavelength and much slower speed. During its interaction with the delamination, S_0 mode with long wavelength appeared due to mode conversion. A_0 waves experience noticeable attenuation from material damping.

Figure 5 shows the zoom-in snapshots of 100-kHz S_0 and A_0 waves interacting with a 20-mm long middle delamination. When S_0 mode interacts with the delamination, the deformation is symmetric about the mid-plane. Flexural motion can be noticed in the laminate layers at the delamination region. The interface was opened and closed at various locations along its length. When A_0 mode interacts with the delamination, top and bottom layers at the delamination follow flexural motion. The delamination interface was also opened and closed by the interrogating wave at various locations along its

length. The contact dynamics at the delamination interface changes the local stiffness periodically and introduce nonlinearity into the sensing signals.

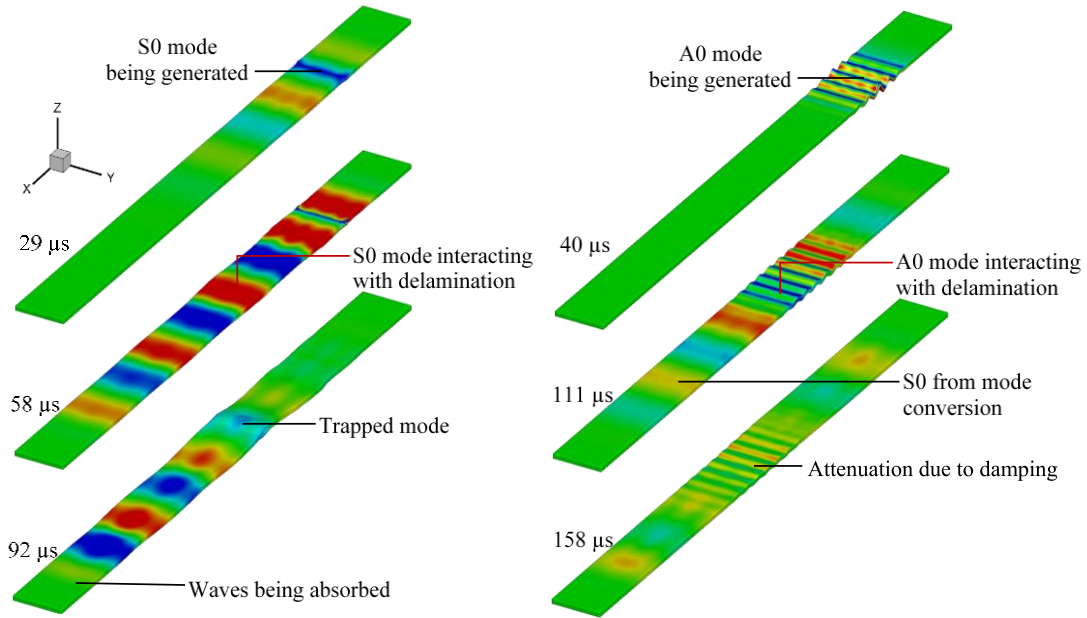


Figure 4: S0 and A0 wave modes generation, propagation, and interaction with the delamination.

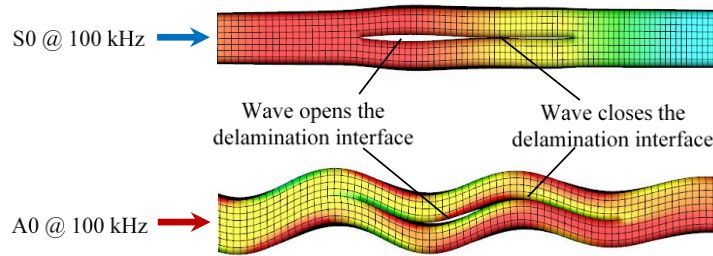


Figure 5: S0 and A0 wave modes opening and closing the middle delamination interface at 100 kHz.

Figure 6a shows the frequency-wavenumber analysis result for S0 wave propagating in a pristine laminate strip. It can be seen that only the generated S0 wave appeared in the wavenumber domain. Figure 6b shows the case of A0 wave propagation in the pristine strip. Again, only generated A0 mode exist. Figure 6c presents the result for S0 wave propagation in a delaminated plate. It can be seen that slight amount of high frequency components appeared. But the nonlinear higher harmonic generation effect is not obvious for such a case. Nevertheless, the result shown Figure 6d indicates that A0 mode is more sensitive to the delamination in terms of nonlinear effect. Distinctive higher harmonic components appeared at 200 kHz, 300 kHz, and 400 kHz. In addition, A0 mode incident wave was mode converted to S0 wave mode. And the higher harmonics appeared as S0 mode at 200 kHz, while mode converted to A1 mode at 300 kHz and 400 kHz. Thus, it can be concluded that at a certain interrogating frequency, different wave modes will exhibit different levels of nonlinear sensitivity.

In order to demonstrate the influence of the excitation frequency on the signal nonlinearity, numerical simulations were also carried out at 200 kHz. Figure 7 presents the frequency-wavenumber analysis of the sensing signals. Figure 7a shows the 200 kHz S0 wave interaction with the delamination. Compared with Figure 6c, it is evident that, at 200 kHz, the nonlinear higher harmonics are more obvious and much stronger than the case of 100 kHz S0 wave incidence case. Thus, for a certain wave mode, its frequency also plays a key role for generating the nonlinear phenomena. Higher harmonic components ride on the S1 mode dispersion curve, indicating a mode conversion to higher order wave modes. It should be noted that, at 200 kHz, two antisymmetric waves, A0 and A1, are both possible in the incident wave field. The in-plane line force excitation couples better with the A1 mode shape as shown in Figure 2. Thus, Figure 7b shows that A1 mode dominates in the propagating waves. Higher harmonics of S1 mode are also quite obvious.

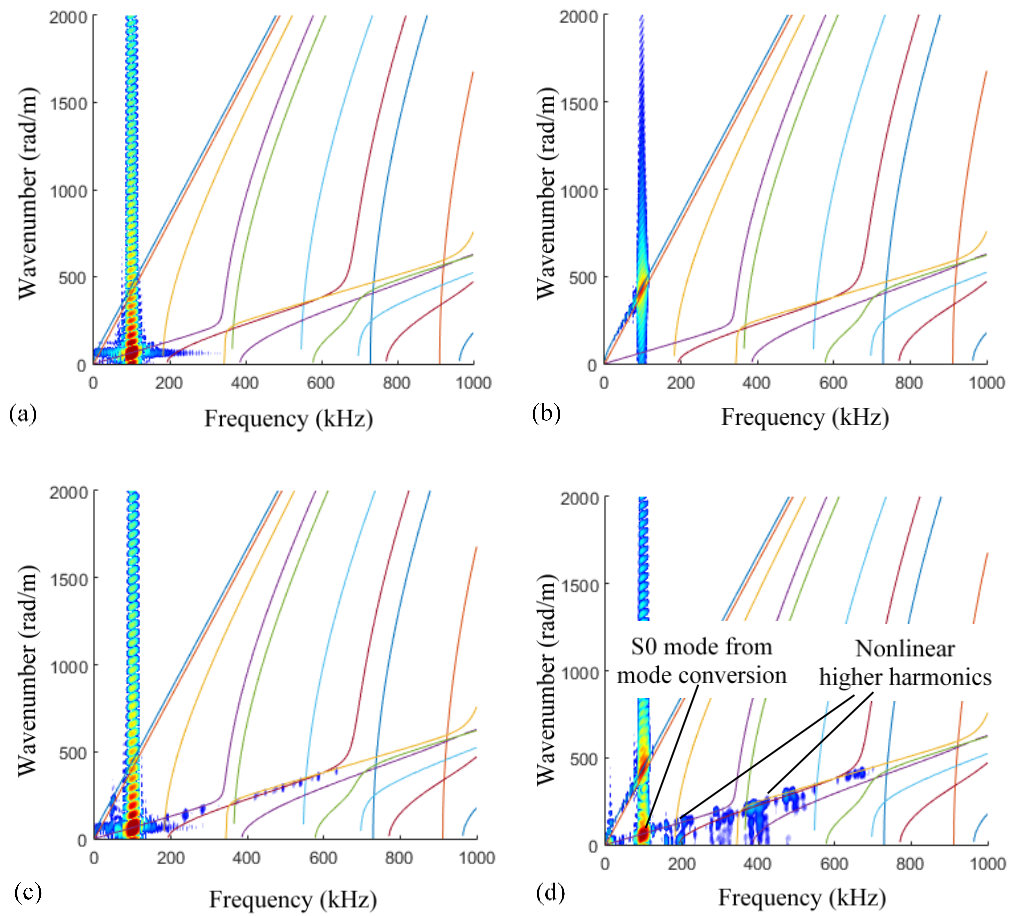


Figure 6: Frequency-wavenumber analysis of wave interaction with middle delamination at 100 kHz: (a) S0 wave propagation in a pristine strip; (b) A0 wave propagation in a pristine strip; (c) S0 wave propagation in a delaminated strip; (d) A0 wave propagation in a delaminated strip. Note the distinctive phenomena of mode conversion and higher harmonic generation.

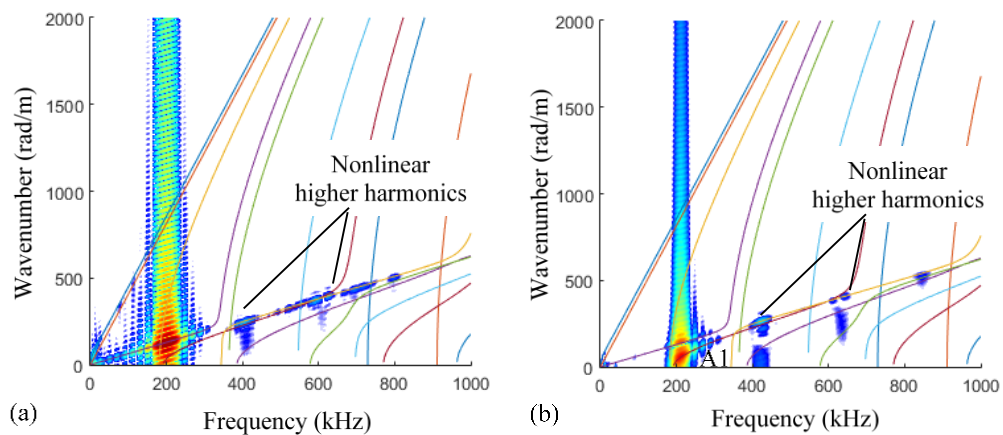


Figure 7: Frequency-wavenumber analysis of wave interaction with middle delamination at 200 kHz: (a) S0 wave propagation in a delaminated strip; (b) A1 wave propagation in a delaminated strip. Note the distinctive phenomenon of higher harmonic generation in both cases.

4.2 Selective wave mode interaction with edge delamination

The different depth where the delamination resides would also influence the wave damage interaction characteristics. In order to investigate this factor, numerical case studies on the wave propagation through edge delamination were carried out. Figure 8 presents S0 and A1 wave modes at 200 kHz interacting with the edge delamination. Trapped motion in the thin upper layer of delamination is quite obvious, accompanied by opening and closing of the delamination interfaces.

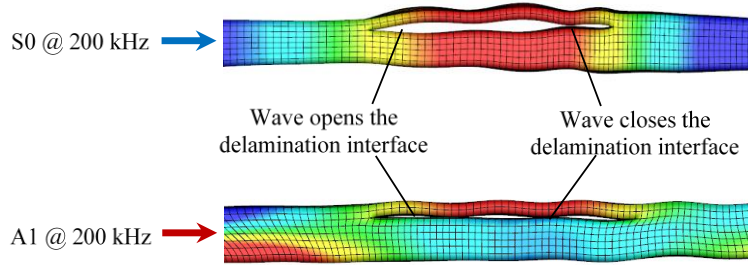


Figure 8: S0 and A1 wave modes opening and closing the edge delamination interface at 200 kHz.

Figure 9 presents the frequency-wavenumber analysis results of wave interaction with edge delamination at 200 kHz. Figure 9a shows that after S0 wave interacted with the edge delamination, obvious higher harmonic components appeared as S1 wave mode, presenting relatively high sensitivity. On the other hand, after A1 mode interacted with the edge delamination, slight second higher harmonic at 400 kHz of S1 mode appeared. The results from both the middle and edge delamination case studies show that S1 mode in the higher harmonic component may serve as a good indicator of the appearance of the delamination.

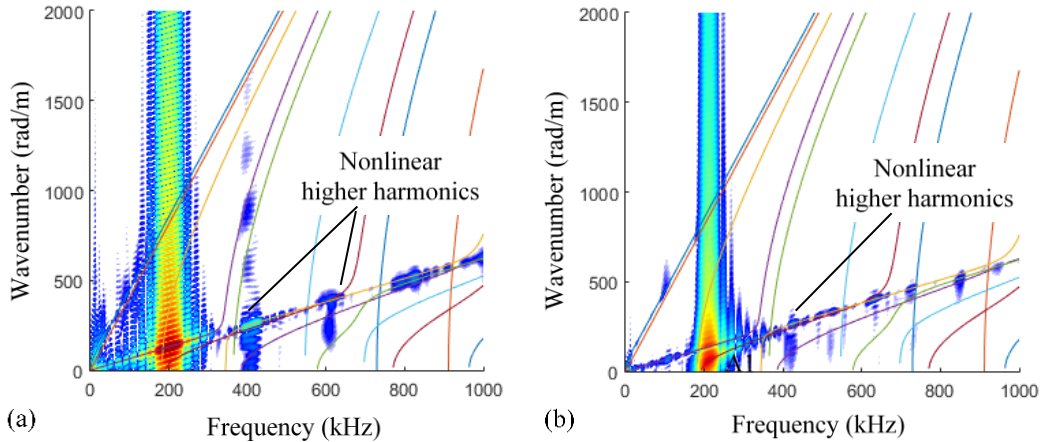


Figure 9: Frequency-wavenumber analysis of wave interaction with edge delamination at 200 kHz: (a) S0 wave propagation in a delaminated strip; (b) A1 wave propagation in a delaminated strip. Note the distinctive phenomenon of higher harmonic generation in both cases.

4.3 Size effect on the nonlinear interaction

The size of the delamination directly influences its interaction with guided waves. In order to investigate the size effect during the nonlinear interactions, numerical case studies of 200-kHz S0 wave propagation through middle delamination of various sizes were carried out. The delamination size a takes the values from 2.5 mm up to 40 mm. The nonlinearity of the signals was measured by the nonlinear index (NI) based on the wave energy ratio:

$$NI = \sqrt{\frac{A_{f_2} + A_{f_3} + A_{f_4}}{A_{f_1}}} \quad (1)$$

where A_{f_1} represents the spectral amplitude of the wave component at the excitation frequency, while A_{f_2} , A_{f_3} , and A_{f_4} are the spectral amplitude of the wave components at the second, third, and fourth higher harmonics.

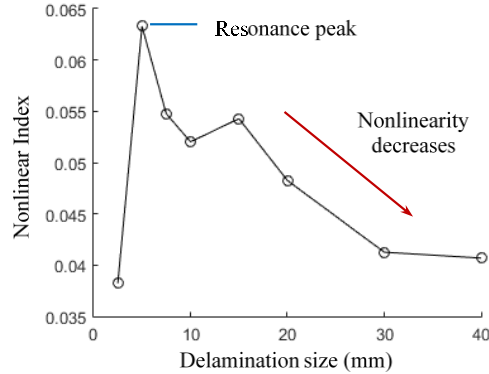


Figure 10: Sensing signal nonlinearity changing with delamination size.

The sensing signals picked up 300 mm away from the wave source was used to generate the nonlinearity trend plots. Intuitively, the damage should impose stronger effects while its size grows. However, the results shown in Figure 10 do not agree with such common sense. The nonlinear index is very small when the delamination is only 2.5-mm long. When it grows to 5-mm long, the index climbed to a high value, indicating the nonlinearity of the signal is quite strong. However, beyond this value, as the delamination size increases, the nonlinear trend starts to decrease. The *NI* peak seems to show a local nonlinear resonance phenomenon.

4.4 Amplitude effect on the nonlinear interaction

It is an important fact that the delamination interfaces are not ideally smooth and perfectly kissing each other. In contrast, the reality is that distributed initial closures and openings exist due to the roughness of the delamination interfaces. The consideration for the initial status of the delineation is critical, because the amplitude of the excitation may play a significant role during the nonlinear interaction. Below a certain threshold, barely noticeable nonlinear effects may be found, i.e., the nonlinear response may heavily depend on the excitation amplitude. Above a certain limit, the nonlinearity of a sensing signal may saturate.

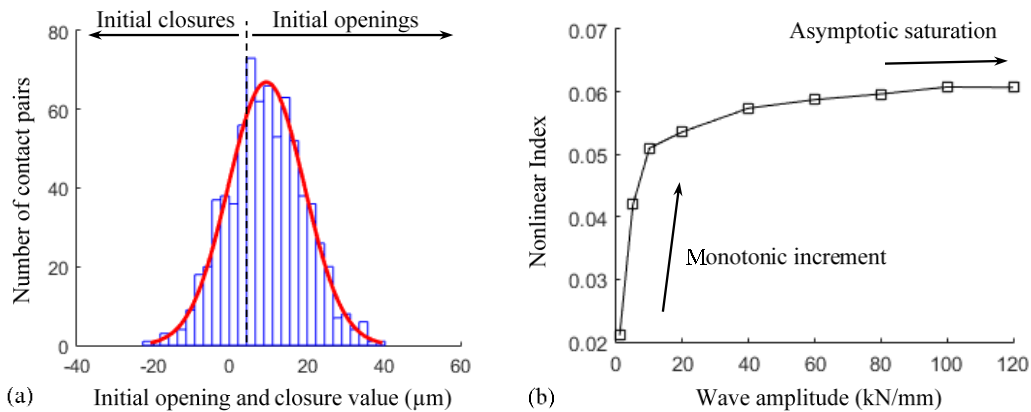


Figure 11: Amplitude effect on the nonlinear interaction: (a) normal distribution of initial openings and closures at the delamination interface; (b) sensing signal nonlinearity changing with excitation amplitude.

Figure 11a shows the status of initial openings and closures at the delamination interface, which was assumed to follow a normal distribution with a mean of 10 μm and a variance of 10 μm . The majority of the delamination area was initially open, with the contact pairs separated from each other. Initial closures also exist at certain locations, representing residual contact stresses acting between these contact pairs. Figure 11b shows that low amplitude excitation would only introduce very weak nonlinearity into the sensing signals. As the excitation amplitude grows, a larger number of contact pairs would be involved in the contact dynamic interactions between the interfaces. Thus, the nonlinearity of the sensing signals would increase. Beyond certain value, the excitation amplitude would engage all the contact pairs in the nonlinear interaction procedure. Thus, the nonlinearity of the signal will approach an asymptotic value, indicating a nonlinear saturation status.

5. CONCLUDING REMARKS

In this study, a parallel LISA numerical model was deployed to study the nonlinear interactions between ultrasonic guided waves and delamination in composite laminate plates. This contact dynamic algorithm is based on the penalty method. A Coulomb friction model was integrated to capture the stick-slip contact motions between the delamination surfaces. The LISA procedure was parallelized via the CUDA technology and executed on powerful graphic cards.

Numerical case studies were conducted on selective guided wave modes interaction with middle and edge delamination. A unidirectional laminate strip LISA model with absorbing boundaries was tailored for the target problem. At 100 kHz, A0 mode showed much higher sensitivity than S0 mode, presenting strong higher harmonic components, while the nonlinear effect in the S0 mode case was weak. Thus, it can be concluded that at a certain excitation frequency, different wave modes have different capability in triggering the CAN. Both S0 and A0 waves were observed to open and close the delamination interface along its length. Distinctive mode conversion phenomena happened between the incident A0 wave mode and the S0 mode at the fundamental frequency as well as A1 mode at higher harmonics. At 200 kHz, S0 and A1 modes were dominant from the line force excitation. The 200-kHz S0 wave case showed much stronger nonlinear effect than that of the 100-kHz case. Thus, it is apparent that for the same wave mode, different sensitivity can be achieved at different interrogation frequencies. The interaction between guided waves and edge delamination was also investigated. Remarkable nonlinear higher harmonic components were present in both S0 and A1 incident case. Mode conversion to S1 wave mode at the higher harmonics may serve as a good indicator for the presence of edge delamination. In this case, S0 mode showed stronger nonlinear effect than A1 mode. The size effect of the nonlinear interactions was investigated by changing the length of the middle delamination and measuring the nonlinearity of the sensing signals using a nonlinear index. It was found that the nonlinearity of the signal did not follow the common intuition that the damage effects would become stronger as the damage size grows. The nonlinearity showed a resonance behavior, peaking at a 5-mm long delamination, while decaying as the size grows further. The roughness of the delamination interfaces were depicted by the initial openings and closures of the contact pairs. It was found that the nonlinear effect is amplitude dependent. In general, when the excitation amplitude is low, merely very weak nonlinearity may arise. The nonlinear effects would become stronger as the excitation amplitude increases. A saturation level exists, engaging all the contact surface into the interaction. The nonlinearity of the signal will then approach an asymptotic value.

For future work, experimental validation and comparison of the proposed contact LISA model should be conducted. The nonlinear resonance effect for various damage sizes, interrogation frequencies, and excitation amplitudes should be investigated.

ACKNOWLEDGEMENTS

The support from the National Natural Science Foundation of China (contract number 51605284) is thankfully acknowledged.

REFERENCES

- [1] Z. Su, C. Zhou, M. Hong, L. Cheng, Q. Wang and X. Qing, "Acousto-ultrasonics-based fatigue damage characterization: linear versus nonlinear signal features," *Mechanical Systems and Signal Processing*, vol. 45, no. 1, pp. 225-239, 2014.
- [2] D. Dutta, H. Sohn, K. A. Harries and P. Rizzo, "A nonlinear acoustic technique for crack detection in metallic structures," *Structural Health Monitoring, An International Journal*, vol. 8, no. 3, pp. 251-262, 2009.
- [3] H. Sohn, D. Dutta, J. Yang, H. Park, M. DeSimio, S. Olson and E. Swenson, "Delamination detection in composites through guided wave field image processing," *Composite Science and Technology*, vol. 71, pp. 1250-1256, 2011.
- [4] Z. Tian, L. Yu and C. Leckey, "Rapid guided wave delamination detection and quantification in composites using global-local sensing," *Smart Materials and Structures*, vol. 25, no. 1, pp. 0-11, 2016.

- [5] R. Soleimanpour, C. Ng and C. Wang, "Higher harmonic generation of guided waves at delaminations in laminated composite beams," *Structural Health Monitoring - An International Journal*, vol. doi: <http://dx.doi.org/10.1177/1475921716673021>, pp. 1-18, 2016.
- [6] R. Soleimanpour and C. Ng, "Locating delaminations in laminated composite beams using nonlinear guided waves," *Engineering Structures*, vol. 131, pp. 207-219, 2017.
- [7] N. Yelve, M. Mitra, P. Mujumdar and C. Ramadas, "A hybrid method based upon nonlinear Lamb wave response for locating a delamination in composite laminates," *Ultrasonics*, vol. 70, pp. 12-17, 2016.
- [8] N. Yelve, M. Mitra and P. Mujumdar, "Detection of delamination in composite laminates using Lamb wave based nonlinear method," *Composite Structures*, vol. 159, pp. 256-266, 2017.
- [9] Y. Shen and V. Giurgiutiu, "WaveFormRevealer: An analytical framework and predictive tool for the simulation of multi-modal guided wave propagation and interaction with damage," *Structural Health Monitoring: An International Journal*, vol. 13, no. 5, pp. 491-511, 2014.
- [10] Y. Shen and V. Giurgiutiu, "Predictive modeling of nonlinear wave propagation for structural health monitoring with piezoelectric wafer active sensors," *Journal of Intelligent Material Systems and Structures*, vol. 25, no. 4, pp. 506-520, 2013.
- [11] S. Hirose, "2-D Scattering by a crack with contact-boundary conditions," *Wave Motion*, vol. 19, no. 1, pp. 37-49, 1994.
- [12] K. Yamanaka, Y. Ohara, M. Oguma and Y. Shintaku, "Two-dimensional analyses of subharmonic generation at closed cracks in nonlinear ultrasonics," *Applied Physics Express*, vol. 4, no. 7, pp. 1-3, 2011.
- [13] P. Delsanto, T. Whitcombe, H. Chaskelis and R. Mignogna, "Connection machine simulation of ultrasonic wave propagation in materials. I: The one-dimensional case," *Wave Motion*, vol. 16, no. 1, pp. 65-80, 1992.
- [14] P. Delsanto, R. Schechter, H. Chaskelis, R. Mignogna and R. Kline, "Connection machine simulation of ultrasonic wave propagation in materials. II: The two-dimensional case," *Wave Motion*, vol. 20, no. 4, pp. 295-314, 1994.
- [15] P. Delsanto, R. Schechter and R. Mignogna, "Connection machine simulation of ultrasonic wave propagation in materials III: The three-dimensional case," *Wave Motion*, vol. 26, no. 4, pp. 329-339, 1997.
- [16] K. Nadella and C.E.S. Cesnik, "Local interaction simulation approach for modeling wave propagation in composite structures," *CEAS Aeronautical Journal*, vol. 4, no. 1, pp. 35-48, 2013.
- [17] K. Nadella and C.E.S. Cesnik, "Effect of piezoelectric actuator modeling for wave generation in LISA," in *SPIE Smart structures and NDE*, San Diego, 2014.
- [18] M. Obenchain, K. Nadella and C.E.S. Cesnik, "Hybrid global matrix/local interaction simulation approach for wave propagation in composites," *AIAA Journal*, vol. 53, no. 2, pp. 379-393, 2014.
- [19] Y. Shen and C.E.S. Cesnik, "Hybrid local FEM/global LISA modeling of damped guided wave propagation in complex composite structures," *Smart Materials and Structures*, vol. 25, no. 9, pp. 1-20, 2016.
- [20] P. Packo, T. Bielak, A. B. Spencer, T. Uhl, W. J. Staszewski, K. Worden, T. Barszcz, P. Russek and K. Wiatr, "Numerical simulations of elastic wave propagation using graphical processing units -- Comparative study of high-performance computing capabilities," *Computer methods in applied mechanics and engineering*, vol. 290, no. 1, pp. 98-126, 2015.
- [21] M. Scalerandi, V. Agostini, P. P. Delsanto, K. V. D. Abeele and P. A. Johnson, "Local interaction simulation approach to modelling nonclassical, nonlinear elastic behavior in solids," *Journal of Acoustical Society of America*, vol. 113, no. 6, pp. 3049-3059, 2003.
- [22] P. Delsanto, A. Gliozzi, M. Hirsekorn and M. Nobili, "A 2D spring model for the simulation of ultrasonic wave propagation in nonlinear hysteretic media," *Ultrasonics*, vol. 44, no. 3, pp. 279-286, 2006.
- [23] M. Scalerandi and V. Agostini, "Simulation of the Propagation of Ultrasonic Pulses in Nonlinear and/or Attenuative Media," *Journal of Computational Acoustics*, vol. 10, no. 3, pp. 275-294, 2002.
- [24] Y. Shen and C.E.S. Cesnik, "Modeling of nonlinear interactions between guided waves and fatigue cracks using local interaction simulation approach," *Ultrasonics*, vol. 74, pp. 106-123, 2017.
- [25] Y. Shen and V. Giurgiutiu, "Effective non-reflective boundary for Lamb waves: Theory, finite element implementation, and applications," *Wave Motion*, vol. 58, pp. 22-41, 2015.